Advances in Science and Technology Vol. 92 (2014) pp 226-231
Online available since 2014/Oct/31 at www.scientific.net

doi:10.4028/www.scientific.net/AST.92.226

Submitted: 06.05.2014
Accepted: 04.07.2014

Mould Fluxes Viscosity and Surface Tension Influence on the Wear Mechanisms of Al_2O_3-C Nozzle

BRANDALEZE Elena[1, a*], PEIRANI Valeria[1, b] and AVALOS Martina[2, c]

[1] Metallurgy Department-DEYTEMA, Universidad Tecnológica Nacional, Colón 332, (2900) San Nicolás, Argentina

[2]IFIR, Universidad Nacional de Rosario, Ocampo y Esmeralda - Ocampo 210 bis, (2000) Rosario, Argentina

[a]ebrandaleze@frsn.utn.edu.ar, [b]vpeirani@frsn.utn.edu.ar, [c]avalos@ifir-conicet.gob.ar

Keywords: nozzle, wear, mould fluxes, physical properties, EBSD

Abstract. A deep understanding of the mould flux effect on the wear mechanisms of Al_2O_3-C nozzles (AG) is relevant to avoid premature damage and to decrease the cost of black refractories in the industry. In this paper, a post mortem study on a nozzle was carried out to identify the causes of the wear mechanisms during the continuous casting of billets. Physical properties such as viscosity and surface tension of the mould fluxes were determined at operation temperature (1550ºC), in order to correlate with microstructural results obtained by light and scanning electron microscopy (SEM). Also dihedral angle ϕ measurements were carried out at high magnification by SEM. Applying EDS analysis the infiltrated mould flux chemical composition was determined. The study was completed by EBSD. The EBSD technique contributed to increase the knowledge on wear mechanisms because of the possibility of identifying and localizing phases together with crystalline condition. The phases, the grain orientations and the properties of grain boundaries, have a large influence on the corrosion behaviour. Therefore, it is essential to have a characterization technique that can provide information such as: grain size, orientation, misorientation angle and the present phases. In this context, EBSD can provide relevant information on crystallographic and structural analysis of AG nozzle including the insert of ZrO_2-C.

Introduction

The requirements for submerged nozzles are particularly harsh. They need to have good thermal shock and chemical attack resistances during the nozzle immersion into molten steel and mould flux at 1530ºC, to prevent expensive production losses during service interruptions. A nozzle with optimum performance in relation to the above requirements is provided by a composite refractory material of alumina-graphite (Al_2O_3-C) bonded by a phenolic resin. The aggressive nature of the mould fluxes in contact with the alumina-graphite material causes localized corrosion problems at the flux line. For this reason, the nozzles include an insert of a zirconia-graphite (ZrO_2-C) to protect the vulnerable zone from chemical attack.

It is known that capillaries, such as open pores and microcracks are the main channels of initial mould flux penetration into a refractory [1, 2]. The evolution of the molten flux physical properties such as viscosity and surface tension in contact with the refractory oxide grains constitutes another important factor to take into account in the interpretation of the corrosion mechanisms. Moreover it is also necessary to consider the refractory texture and microstructure. The evolution of the microstructure during penetration by a liquid can be interpreted on the basis of the interfacial energy balance (see Eq.1) [3]:

$$\gamma_{gb} = 2\,\gamma_{sl}\cos(\phi/2) \quad (1)$$

Where: γ_{gb} and γ_{sl} are the grain boundary energy and solid/liquid interface energy respectively, and ϕ the dihedral angle.

In Table 1 the conditions for penetration or no penetration into the refractory grain boundaries, described by Lee and Zhang in [3] are summarized.

Table 1. Penetration conditions in relation with the ratio γ_{gb}/γ_{sl}.

Ratio γ_{gb}/γ_{sl}	Penetration condition
≥ 2	Liquid can penetrate into de grain boundaries at equilibrium
$>\sqrt{3}$	Liquid surrounds all the 3 grain edges as a continuously connected phase
between 1 and $\sqrt{3}$	Liquid can partially penetrate along grain boundaries
<1	No penetration will occur

In this paper a post mortem study on a nozzle used for billet casting, was carried out with the objective to identify the wear mechanisms present during service in the insert of ZrO_2-C. The structural aspect was studied by different microscopy techniques such as light microscopy and scanning electron microscopy (SEM). Also the dihedral angle ϕ was measured directly from SEM images. The chemical composition of the penetrated flux and the oxide grains was determined by energy dispersive spectroscopy (EDS). The results were correlated with the molten flux physical properties calculated by theoretical models at 1550ºC. In this case surface tension (γ) and viscosity (η) were estimated by the theoretical model described by Mills et al. [4]. The EBSD technique also contributed to increase the knowledge on wear mechanisms because of the possibility to identify and localize phases from crystalline conditions. Nozzles possess a complex crystal structure coupled with anisotropic material properties. The phases, the crystal orientations of grains and grain boundary properties, have a large influence on the chemical resistance properties of these materials; for what it is important to introduce an appropriate characterization technique. In this context, EBSD can provide relevant information on crystallographic and structural analysis on AG nozzle including the insert material of ZrO_2-C [5, 6].

Experimental

The study was carried out on two AG nozzle samples with ZrO_2-C insert: a post mortem sample identified such as (PM) and a reference sample identified as (AR).The chemical compositions of both samples were determined by atomic emission analysis (see Table 2).

Table 2. Chemical composition of the AG nozzles.

Oxide	Al_2O_3-C body [wt %]		ZrO_2-C insert [wt %]	
	AR	PM	AR	PM
SiO_2	5.9	3.4	0.5	-
Al_2O_3	88.0	91.0	0.1	0.1
B_2O_3	2.6	2.7	-	-
CaO	-	-	4.0	4.0
ZrO_2	3.5	2.8	94.3	94.0
HfO_2	-	-	1.8	1.5
C	24.0	22.0	16.9	16.0

Density and apparent porosity of the nozzle were determined by Archimedes method. The loss on ignition (LOI) of the body and insert materials, was obtained by experimental tests at 950 ºC during 2 h and were correlated with results of thermogravimetry (TG) using a Shimadzu DTG 60. The microstructure was observed by a light microscope Olympus GX51 with an image analyzer system LECO IA32 and with a SEM-FEI Quanta 200. The study includes the phase's semi quantitative analysis by EDS and mapping of the element distribution. Also the dihedral angle ϕ was measured applying SEM. The crystallography and chemical composition of aggregates in the refractory material was determined by EBSD - EDS (TSL -EDAX) system analysis. EBSD is a surface technique that requires highly polished samples in order to acquire diffraction data

('Kikuchi patterns'). The nozzles samples were treated using a conventional polishing sequence and a two hours final step of 0.05-µm colloidal silica in vibratory polisher. Mold flux composition is a complex oxide system (See Table 3) with a basicity index IB = 0.70. The rest to complete 100 wt% is carbonaceous material.

Table 3. Chemical composition of the mould flux F in [wt %].

SiO_2	Al_2O_3	CaO	Na_2O	MgO	F	TiO_2	MnO	Fe_2O_3	K_2O	P_2O_5
31.6	14.4	22.2	3.7	2.1	2.6	1.0	0.3	3.4	1.6	0.5

Viscosity and surface tension of the flux and of the infiltrated liquid into nozzle refractory material were determined through theoretical models (based on the chemical composition). The critical temperatures (softening, hemisphere and fluidity) were determined by hot stage microscopy (HSM).

Results and Discussion

Physical properties of the nozzle and the mould flux. As it is known, apparent porosity (P_a) and density (δ) of the nozzle refractory material have important influence on the mould flux infiltration and their chemical attack. Results of those physical properties are showed in Table 4. A low densification is observed in the PM sample and it is developed during the preheating process and hours of use. The δ results are consistent with the LOI values obtained by experimental test on both nozzles. The mass loss results are consistent with the TG curve up to 1450 ºC (Fig. 1) on AR sample. The AR sample mass loss during heating occurs in two steps and at temperatures lower than 850 ºC. This is due to pyrolysis reactions of the phenolic resin binder. In this type of refractory materials the bond contains phenolic resin and different types of carbonaceous particles such as: carbon black, calcined anthracite coal and graphite flakes, in order to avoid cracking and thermal shock failures [7]. At temperatures higher than 850 ºC, no loss of mass was detected. The critical temperature of the flux F, established by HSM, shows that at 1255ºC it is fully fluid (Table 5). The viscosity (η) of flux F estimated by a theoretical model at 1550ºC is 4.4 dPa.s, which is considered a high viscosity fluid. A high viscosity penetrating liquid decreases infiltration tendency in the refractory [3].

Table 4. Physical properties of nozzles.

Sample	δ [g/cm^3]	P_a [%]	LOI [%]
AR	2.5	15.8	23
PM	2.6	14.8	21

Table 5. Critical temperatures of flux F.

Sample	$T_{softening}$ [ºC]	$T_{hemisphere}$ [ºC]	$T_{fluidity}$ [ºC]
F	1174	1187	1255

Surface tension of flux F decreases when temperature increase, as it is showed in Fig. 2. Another important factor to consider is the basicity index IB of the flux that is relatively low (0.7). Fluxes with low basicity index in contact with the ZrO_2 stabilized with CaO have lower penetration temperature and promotes insert corrosion [3].

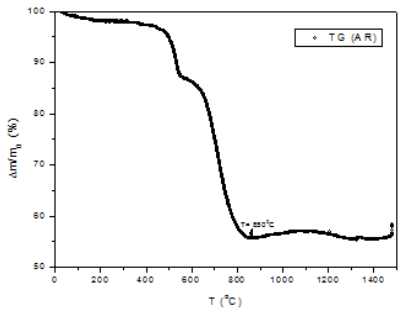

Figure 1. AR mass loss obtained by TG curve

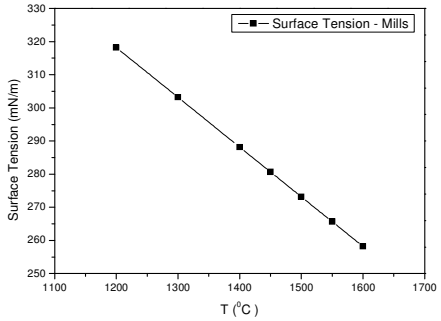

Figure 2. Surface tension with temperature

Comparative structural study. The structure of the AR y PM samples were observed by light microscopy and electron microscopy (SEM) to compare the effect of the molten flux on the nozzle. The samples were observed in both zones: the body of Al_2O_3-C and the insert of ZrO_2-C. Fig. 3 shows the aspect of the structure in the insert zone of the sample PM (near the interface with adhered flux layer). In PM sample, ZrO_2 grains cracked by thermal stresses are observed. As reference, Fig. 4 shows the structure of the insert material in the AR nozzle.

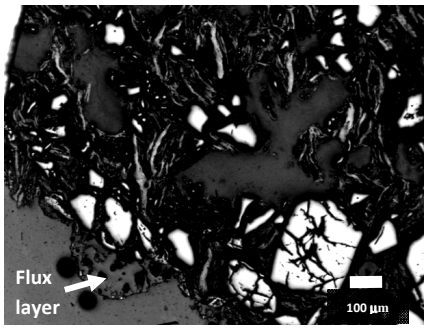

Figure 3. Structure of the insert in PM sample.

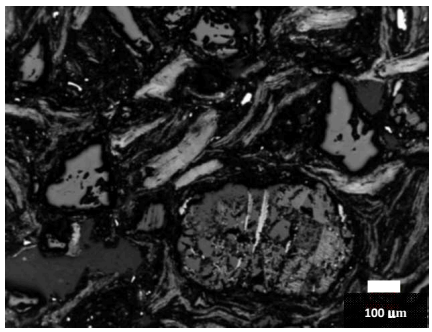

Figure 4. Structure of the insert in AR sample.

Comparing both microstructures allows verifying that in the insert of the PM sample there are loss of both ZrO_2 grains and binder near the surface. However, the graphite flakes are present. Also the SiO_2 grains have decreased by reaction with the alkalis of the mould flux [7]. The holes and microcracks represent channels that intensify the infiltration tendency at the hot face.

Veins of flux infiltrations into refractory material and corroded ZrO_2 grains were visualized in different zones of the sample surface. Isolated fragments of the ZrO_2 aggregates were present into the flux layer near the interface with nozzle surface. The structural observations by SEM are reported in Fig. 5. The image of the studied zone is presented, indicating with 1 and 2 the areas where the EDS analyses were carried out. The evolution of the chemical composition in the adhered flux layer was determined by sequential analysis. The results show considerable decreases of SiO_2 and CaO in the flux layer in comparison with the original chemical composition of the flux. On the other hand, an important increase on Na and F contents was measured near the interface flux layer-nozzle. Flux chemical composition changes cause viscosity and surface tension variations during service. The elements distribution in the area was visualized by EDS maps: Zr indicates ZrO_2 grains in the refractory or fragments of grains in the flux layer (like the indicated by 2). Furthermore, C allows identifying graphite flakes and carbon binder. Although the flux layer contains oxides of Si, Na, Ca, Mg, Al and F compounds, in Fig. 5 only maps of Si, Na and F were included.

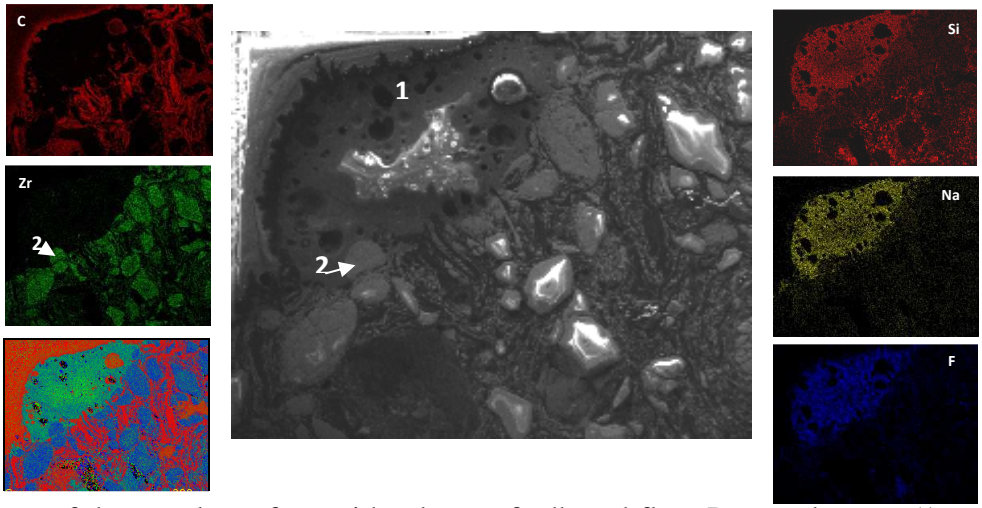

Figure 5. Zone of the nozzle surface with a layer of adhered flux. Punctual zones (1 and 2) of EDS analysis and element mapping images of C, Zr, Si, Na and F are showed.

Down on the left in Fig. 5 a map composed by all the elements detected is presented in order to make clear de differences in the chemical distribution. The fragment of the ZrO_2 grain (indicated as 2) in the flux layer corroborates the corrosion mechanism by chemical attack due to the molten flux [2, 3]. The aggregate detachment was caused by liquid flux penetration through grain boundaries.

It was possible to determine the evolution of the viscosity and surface tension between the original flux and the infiltrated liquid at 1550 ºC to verify the effect of both properties on corrosion mechanism due to infiltration. The viscosity of the flux decreases from 4.4 dPa.s in the original flux to 0.21 dPa.s in the infiltrated flux. The surface tension γ also presents changes at 1550 ºC: 270 mN/m for the original flux and 470 mN/m in the flux layer near the interface. In the infiltrated liquid the value is ≈ 430 mN/m (see, Fig. 6). Both values are considered only an approximation because they are estimated on the basis of semi-quantitative EDS results. The liquid flux chemical composition evolution during service justifies the changes observed on the physical properties and liquid infiltration phenomena into the nozzle insert and ZrO_2 grain boundaries.

The ratio γ_{gb}/γ_{sl} described was calculated in the infiltrated grains of ZrO_2 by the dihedral angle ϕ measured by SEM. The correlation of this ratio with the ϕ dihedral angle was considered for two conditions: $60^0<\phi<120^0$ and $\phi > 120^0$. Values of $1 < \gamma_{gb}/\gamma_{sl} < 2$ were calculated for the last condition (Fig.7) corroborating both conditions: partially liquid flux penetration along ZrO_2 grain boundaries and liquid surrounding all the 3 grain edges as a continuously connected phase.

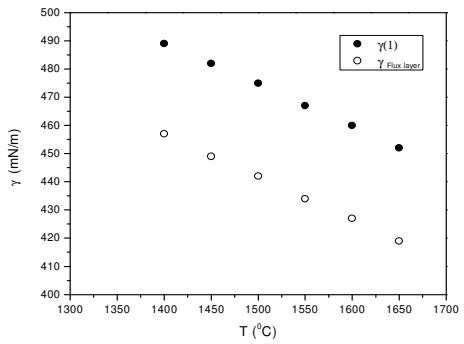

Figure 6. Surface tensions of the flux in zone (1) and in the flux layer interface with the nozzle insert.

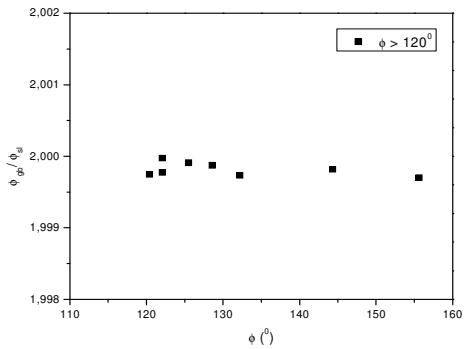

Figure 7. Ratio γ_{gb}/γ_{sl} in function of angle ϕ determined by SEM on ZrO_2 grains.

According to Eustathopoulus et al. [1] a melt can penetrate into a polycrystalline solid through two types of defects: 3D defects consisting in a network of open pores, and 2D defects consisting in a network of grain boundaries. Both, the capillary infiltration and the grain boundary wetting contribute to refractory corrosion and degradation. The infiltration increases the solid/melt area and thus promotes refractory dissolution in the melt, what might explain the increase of ZrO_2 content in the flux layer near the interface up to 1.16 % wt, detected by the EDS analysis. When the melt reaches the inner part of the solid the grain boundary penetration starts causing the grains to be detached and transferred to the melt. At high temperature and prolonged contact time, aluminum silicate compounds produce the ZrO_2 destabilization together with volume expansion [2]. The mentioned mechanism has been identified at the outer reaction layer of the grain.

In this work the EBSD technique combined with EDS was also useful to corroborate the corrosion mechanisms in the PM nozzle insert. Fig. 8 shows a SEM image of a ZrO_2 grain heavily attacked. The Inverse Pole Figure (IPF) map of Fig. 9 combined with the Image Quality (IQ) map of Fig. 10 indicates that the outer part of the grain could not be indexed probably because the cubic crystal structure was gradually destabilized and changed to a tetragonal crystalline structure. The chemical maps of Zr and Si are shown in Figures 11 and 12. The Zr shows homogenous distribution in coincidence with the grain limits; meanwhile the Si and Ca are more intense in the non-indexed areas.

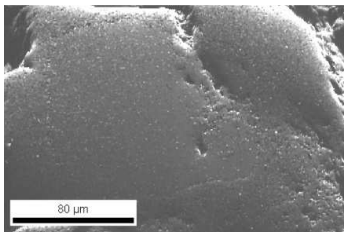

Figure 8. Detector image of ZrO_2 particle.

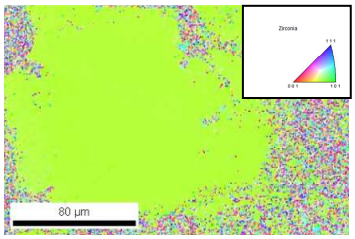

Figure 9. IPF of ZrO_2 particle corresponding to Fig. 8.

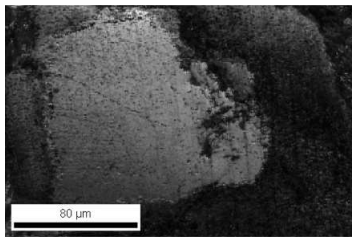

Figure 10. IQ of ZrO_2 particle corresponding to Fig. 8.

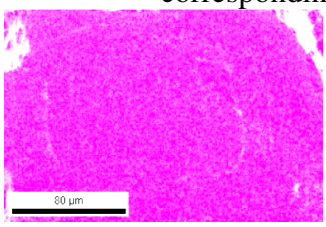

Figure 11. Zr content map of ZrO_2.

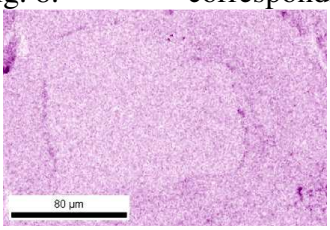

Figure 12. Si content map of ZrO_2.

Summary

During preheating of the nozzle and during service in continuous casting, the binder mass loss promotes channels formation for flux penetration. For this reason it is necessary to develop an adequate preheating profile in the industrial plants. The decrease of viscosity and surface tension variation of the flux, due to chemical composition evolution at processing conditions, and a low value of basicity index (IB = 0.7) determine the corrosion mechanisms on submerged nozzles insert. The infiltration of the liquid between ZrO_2 grain boundaries can be characterized by dihedral angle ϕ measurements by SEM and the estimation of the γ_{gb}/γ_{sl} ratio. In ZrO_2 grains for $\phi > 120^0$ the liquid flux with a viscosity $\eta \sim 0.21$ dPa.s and a surface tension $\gamma \sim 430$ mN/m could surround all the 3 grain edges as a continuously connected phase at 1550 ºC. The EBSD technique showed relevant information on the ZrO_2 corrosion mechanisms: the crystalline structure changes (cubic to tetragonal) due to ZrO_2 destabilization for calcium loss by diffusion.

References

[1] N. Eustathopoulus, R. Parra and M. Sánchez, Role of capillarity in corrosion of refractories by melts, in: C. Díaz, C. Landolt, T. Utigard (Eds.), Copper 2003 - The Hermann Schwarse Symposium on Copper Pyrometallurgy, Vol.: 5, Book 2, 2003, pp. 457-471.
[2] E. Brandaleze, E. Benavidez, V. Peirani, L. Santini, C. Gorosurreta, Impact of free fluor fluxes on nozzle wear mechanisms, Advances Science and Technology, 70 (2010) 205-210.
[3] W.E. Lee, S. Zhang, Melt corrosion of oxide and oxide-carbon refractories, International Materials Reviews, 44 (1999) 77-104.
[4] K.C. Mills, L. Yuan, R.T. Jones, Estimation the physical properties of slags, The Journal of The Southern African Institute of Mining and Metallurgy 111 (2011) 649-657.
[5] J.K. Farrer, J.R. Michael, C.B. Carter, EBSD of ceramic materials, in: A. J. Schwartz, M. Kumar, B. L. Adams (Eds), Electron Backscatter Diffraction in Materials Science, Ch. 24, 2000, pp. 299-318.
[6] E. Benavidez, M.V. Peirani, M. Ávalos, E. Brandaleze, Effects of viscosity and surface tension of free fluorine fluxes on the wear mechanisms of Al_2O_3-C nozzle, UNITECR 2013 Proceeding, (2013) 483-488.
[7] A.J. Dzermejko, Carbonaceous Refractories, in: C. A. Schacht (Eds.), Refractories Handbook – Marcel Dekker, Inc., Ch. 8, 2004, pp. 457-471.

13th International Ceramics Congress - Part F
10.4028/www.scientific.net/AST.92

Mould Fluxes Viscosity and Surface Tension Influence on the Wear Mechanisms of Al_2O_3-C Nozzle
10.4028/www.scientific.net/AST.92.226